

**MICROWAVE ASSISTED PROCESSING OF Zr-DOPED  $\text{CaCu}_3\text{Ti}_4\text{O}_{12}$   
ELECTROCERAMICS**

**by**

**MOHD SYHRIL BIN MOHD SHARIFUDDIN**

**Thesis submitted in fulfilment of the requirements  
for the degree of  
Master of Science**

**June 2007**

## **ACKNOWLEDGEMENT**

I would like to express my sincere appreciation to those who contributed to this thesis, without their help it would not been possible. It is not possible to write such a thesis without being in a privileged research environment, which has continuously been provided by the School of Materials and Mineral Resources Engineering, Universiti Sains Malaysia (USM).

First, I'd like to thank a lot of co-workers have directly or indirectly contributed to this project. I want to acknowledge my high spirited supervisor, Dr. Sabar Derita Hutagalung in the first place or his major contributions to the successful of this project, as well as my co-supervisor, Prof. Dr. Haji Zainal Arifin Ahmad for providing the knowledge base for my future.

I would also like to thank all the staffs, especially Mr. Shahrul, Madam Fong, Mr. Helmi, Mr. Farid, Mr. Rashid, Mr. Mokhtar, Mr. Azam, Mr. Suhaimi and Mrs. Haslina for their technical support, as well as my postgraduate friends, Firdaus, Asraff, Niki Prostomo, Umar Al-Amani, Salimin, Fadzli, Mohd Hasbi, Mahathir Amir, Aye Aye Thant, Aspaniza, Rosmawati, Wan Nur Fadzilah, Nurhidayatullaili, Erfan Suryani, Zunaida and Nadirah who always available for discussions.

Special thanks to my family for their love and continued support. Although I'm sure to forget some of them who contributed to this research, I express the utmost gratitude to all of them that deserve my thanks.

## TABLE OF CONTENTS

	<b>PAGE NUMBER</b>
ACKNOWLEDGEMENTS	ii
TABLE OF CONTENTS	iii
LIST OF TABLES	viii
LIST OF FIGURES	ix
LIST OF ABBREVIATION	xv
LIST OF MAIN SYMBOL	xvi
ABSTRAK	xvii
ABSTRACT	xviii
<b>CHAPTER 1: INTRODUCTION</b>	
1.1    Ceramics Materials	1
1.2    Problem Statement	3
1.3    Research Objective	5
<b>CHAPTER 2: LITERATURE RIVIEW</b>	
2.1    Introduction	6
2.2    Dielectric Materials	6
2.3    Dielectric Properties	6
2.4    Perovskite Structure	10
2.5    CaCu <sub>3</sub> Ti <sub>4</sub> O <sub>12</sub>	12
2.5.1    Grains Boundaries Effect	15
2.5.2    Processing Effect	16
2.5.3    Electrode/sample contact effects	18
2.5.4    Chemical Modifications on CaCu <sub>3</sub> Ti <sub>4</sub> O <sub>12</sub>	20

	2.5.4.1 Isovalent Substitution	20
	2.5.4.2 Acceptor Dopants	24
	2.5.4.3 Donor Dopants	25
2.6	Microwave Heating	27
	2.6.1 Susceptor	30
	2.6.1.1 SiC Susceptor	31
	2.6.1.2 Graphite Susceptor	32
	2.6.2 Effect of Microwave Heating	32
2.7	Concluding Remark	36

### **CHAPTER 3: MATERIALS AND METHODOLOGY**

3.1	Experimental Design	37
3.2	Starting Materials	39
3.3	Processing Steps in Phase I (Using furnace during calcination and sintering)	39
	3.3.1 Composition Formulation	39
	3.3.2 Ball Milling	40
	3.3.3 Calcination	41
	3.3.4 De-agglomeration	44
	3.3.5 Uniaxial Pressing	44
	3.3.6 Sintering	45
3.4	Processing Steps in Phase II (Microwave Oven Route)	46
	3.4.1 Composition Formulation	46
	3.4.2 Ball Milling	47
	3.4.3 Calcination	47
	3.4.3.1 Graphite Susceptor	48

3.4.3.2	Silicon Carbide Susceptor	49
3.4.4	De-agglomeration	50
3.4.5	Uniaxial Pressing	50
3.4.6	Sintering	50
3.5	Sample Preparation and Characterization Techniques	51
3.5.1	X-Ray Diffraction (XRD)	51
3.5.1.1	X-ray Diffraction Principle	51
3.5.2	Scanning Electron Microscope	52
3.5.3	FTIR Analysis	53
3.5.4	Particle Size Analysis	54
3.5.5	Density and porosity determination by Archimedes method	54
3.5.6	Dielectric Properties Measurement	55

## **CHAPTER 4: RESULTS AND DISCUSSION**

4.1	Introduction	57
4.2	Charazterization of Starting Materials	57
4.2.1	Ca(OH) <sub>2</sub> Powder	58
4.2.2	CuO Powder	59
4.2.3	TiO <sub>2</sub> Powder	60
4.2.4	ZrO <sub>2</sub> Powder	61
4.2.5	FTIR Analysis of Hardener	62
4.3	CaCu <sub>3</sub> Ti <sub>4</sub> O <sub>12</sub> Prepared via Solid State Reaction	63
4.3.1	Dielectric Properties of undoped CaCu <sub>3</sub> Ti <sub>4</sub> O <sub>12</sub>	67
4.3.2	Zr-doped CaCu <sub>3</sub> Ti <sub>4</sub> O <sub>12</sub> derived from Furnace Processing	68
4.3.2.1	Phase Analysis of Sintered Pellets	69

	Derived from Furnace Route	
	4.3.2.2 Density and Porosity of Sintered Pellet	70
	Derived from Furnace Route	
	4.3.2.3 Dielectric Properties of Sintered Pellets	71
	Derived from Furnace Route	
	4.3.2.4 Microstructure of Sintered Pellets	72
	Derived from Furnace Route	
4.4	CaCu <sub>3</sub> Ti <sub>4</sub> O <sub>12</sub> Prepared via Microwave Processing	75
	4.4.1 Alumina Crucible as Susceptor in Microwave Processing	76
	4.4.2 Graphite Crucible as Susceptor in Microwave Processing	77
	4.4.2.1 Phase Analysis of Sintered Pellets using Graphite as Susceptor	77
	4.4.3 SiC Crucible as Susceptor in Microwave Processing	79
	4.4.3.1 Phase Analysis of Calcined Powders using SiC as Susceptor	80
	4.4.3.2 Microstructure of Calcined Powders using SiC as Susceptor	86
	4.4.4 Comparison of Calcined Powders from Furnace Route and Microwave Oven	89
	4.4.5 Dielectric Properties of Sintered Pellets Derived from Microwave Heating	91
	4.4.6 Microstructure of Sintered Pellets Derived from Microwave Processing	91

## CHAPTER 5: CONCLUSION AND RECOMMENDATION FOR FUTURE RESEARCH

5.1	Conclusion	93
5.2	Recommendation for Future Research	84
<b>REFERENCES</b>		97
<b>APPENDIX</b>		100
APPENDIX A	Weight of Starting Materials	100
APPENDIX B	Calculation on Starting Materials Needed to Prepare A Batch of 30 gram $\text{CaCu}_3\text{Ti}_4\text{O}_{12}$	101
APPENDIX C	Calculation on Starting Materials Needed to Prepare A Batch of 30 gram $\text{CaCu}_3\text{Ti}_{3.99}\text{Zr}_{0.01}\text{O}_{12}$	102
APPENDIX D	Calculation on Starting Materials Needed to Prepare A Batch of 30 gram $\text{CaCu}_3\text{Ti}_{3.98}\text{Zr}_{0.02}\text{O}_{12}$	103
APPENDIX E	Calculation on Starting Materials Needed to Prepare A Batch of 30 gram $\text{CaCu}_3\text{Ti}_{3.96}\text{Zr}_{0.04}\text{O}_{12}$	104
APPENDIX F	Calculation on Starting Materials Needed to Prepare A Batch of 30 gram $\text{CaCu}_3\text{Ti}_{3.94}\text{Zr}_{0.06}\text{O}_{12}$	105
APPENDIX G	Calculation on Starting Materials Needed to Prepare A Batch of 30 gram $\text{CaCu}_3\text{Ti}_{3.9}\text{Zr}_{0.1}\text{O}_{12}$	106
APPENDIX H	Powder Diffraction File	107
APPENDIX I	Powder Diffraction File	108
APPENDIX J	X-ray Diffraction Pattern	109
APPENDIX K	Powder Diffraction File	110

## LIST OF TABLES

Table 2.1	Dielectric Constant at 25 °C	9
Table 2.2	Relative density versus processing temperature for microwave (MHH) and conventionally processed alumina bars	30
Table 3.1	Weight of starting materials to prepare a 30 gram batch Zr-doped $\text{CaCu}_3\text{Ti}_4\text{O}_{12}$	39
Table 4.1	Results of electrical properties of sintered pellet via microwave heating	91

## LIST OF FIGURES

Figure 2.1	A parallel-plate capacitor (a) when a vacuum is present and (b) when a dielectric material is present	9
Figure 2.2	Several unit cells of $\text{CaCu}_3\text{Ti}_4\text{O}_{12}$ , shown as $\text{TiO}_6$ octahedra, Cu atoms (blue) bonded to four oxygen atoms (red), and large Ca atoms (yellow) without bonds	11
Figure 2.3	Unit cell of body-centered cubic $\text{CaCu}_3\text{Ti}_4\text{O}_{12}$ in the $\text{Im}\bar{3}$ space group	13
Figure 2.4	(a) The real part of the dielectric constant, $\epsilon'$ (T), for two different samples of $\text{CaCu}_3\text{Ti}_4\text{O}_{12}$ . (b) The loss component of the dielectric response, expressed as $\tan \delta$	14
Figure 2.5	(a) The real part, $\epsilon'$ , of the dielectric dispersion at different frequency and (b) plots of $\ln(J/A T^2)$ versus $E^{1/2}$ of three different $\text{CaCu}_3\text{Ti}_4\text{O}_{12}$ ceramic samples measured at room temperature	15
Figure 2.6	SEM photographs of the two $\text{CaCu}_3\text{Ti}_4\text{O}_{12}$ ceramic samples which were sintered for 20 hours and 80 hours	16
Figure 2.7	Frequency dependence of real part of dielectric constant ( $\epsilon_r'$ ) at 225 K for $\text{CaCu}_3\text{Ti}_4\text{O}_{12}$ pellets sintered for different durations at 1100 °C	18
Figure 2.8	a) Frequency dependence of the dielectric constant at room temperature for $\text{CaCu}_3\text{Ti}_4\text{O}_{12}$ sample with different electrodes, (b) Dielectric constant at room temperature for sample (a) with silver paint electrode, (b) annealed in $\text{N}_2$ at 750 °C for 8 hours	19

with silver paint electrode, (c) annealed in N<sub>2</sub> at 750 °C for 8 hours with the Pt electrode, (d) annealed in O<sub>2</sub> at 750 °C for 16 hours with Pt electrode

Figure 2.9	The dielectric constants versus temperature of Zr-doped BaTiO <sub>3</sub> ceramics (a) with 0.8 at.% (b) with 2 at.% and (c) with 5 at.% (frequency = 1 kHz)	21
Figure 2.10	Surface microstructures of Ba <sub>0.4</sub> Sr <sub>0.4</sub> Ca <sub>0.2</sub> TiO <sub>3</sub> specimens with various ZrO <sub>2</sub> contents	21
Figure 2.11	Relative dielectric constant and dielectric loss at 1 kHz as a function of temperature for Ba <sub>0.45</sub> Sr <sub>0.4</sub> Ca <sub>0.15</sub> TiO <sub>3</sub> specimen with various ZrO <sub>2</sub> contents	22
Figure 2.12	(a) Apparent relative permittivity ( $\epsilon'_{app}$ ) (b) loss tangent ( $\tan \delta$ ) of pure and 2 wt.% SiO <sub>2</sub> doped-CaCu <sub>3</sub> Ti <sub>4</sub> O <sub>12</sub> specimens: S-CCTO-1100 (2 wt.% SiO <sub>2</sub> doped, sintered at 1100 °C for 12 hours); S-CCTO-1060 (2 wt.% SiO <sub>2</sub> doped, sintered at 1060 °C for 12 hours); CCTO-1140 (pure, sintered at 1140 °C for 12 hours)	23
Figure 2.13	The dielectric constant of CaCu <sub>3-x</sub> Mn <sub>x</sub> Ti <sub>4</sub> O <sub>12</sub> , (a) x = 0, (b) x = 0.06	25
Figure 2.14	Impedance plots of (a) La2%, (b) V 2%, (c) Cr 2% and (d) Mn2%-doped samples	26
Figure 2.15	Relative dielectric constant data for CaCu <sub>3</sub> Ti <sub>4</sub> O <sub>12</sub> showing the effect of Cu deficiency at room temperature	27
Figure 2.16	Illustration of sample setting for microwave sintering	29
Figure 2.17	Effect of power-dependent microwave absorption on the heating	31

	of SiC, Al <sub>2</sub> O <sub>3</sub> and ZrO <sub>2</sub> powders without any preheater	
Figure 2.18	Microwave heating of graphite	32
Figure 2.19	(a) Sintering temperature dependence, (b) temperature dependence of dielectric constant and dielectric loss of PZT tapes sintered by microwave and conventional sintering	34
Figure 2.20	SEM photograph of BaTiO <sub>3</sub> -1.5 mol% BaB <sub>2</sub> O <sub>4</sub> microwave sintered sample	35
Figure 2.21	Dielectric properties of each sample. (a) Conventional sintering sample without additive, (b) Microwave sintering sample with BaCO <sub>3</sub> + H <sub>3</sub> BO <sub>3</sub>	36
Figure 3.1	Process flow of phase I and phase II	38
Figure 3.2	(a) Jar mill made from alumina, (b) Cylindrical zirconium used as the media	41
Figure 3.3	Alumina crucible used to calcine Ca(OH) <sub>2</sub> -CuO-TiO <sub>2</sub> mixtures in the furnace	42
Figure 3.4	Temperature profile for calcination of undoped CaCu <sub>3</sub> Ti <sub>4</sub> O <sub>12</sub> and Zr-doped CaCu <sub>3</sub> Ti <sub>4</sub> O <sub>12</sub> powder	43
Figure 3.5	Hydraulic hand press machine	45
Figure 3.6	Temperature profile for sintering of undoped CaCu <sub>3</sub> Ti <sub>4</sub> O <sub>12</sub> and Zr-doped CaCu <sub>3</sub> Ti <sub>4</sub> O <sub>12</sub> powder	46
Figure 3.7	Graphite susceptor inside SiC susceptor with SiC powders in between the two susceptor	48
Figure 3.8	Susceptor for microwave heating made from 40 wt.% coarse silicon carbide particles distributed in an alumina cement matrix	49
Figure 4.1	SEM micrograph of Ca(OH) <sub>2</sub>	58

Figure 4.2	Particle size distribution of Ca(OH) <sub>2</sub> powder	59
Figure 4.3	SEM micrograph of CuO	59
Figure 4.4	Particle size distribution of CuO powder	60
Figure 4.5	SEM micrograph of TiO <sub>2</sub>	60
Figure 4.6	Particle size distribution of TiO <sub>2</sub> powder	61
Figure 4.7	SEM micrograph of ZrO <sub>2</sub>	61
Figure 4.8	Particle size distribution of ZrO <sub>2</sub> powder	62
Figure 4.9	FTIR spectra of solution for setting the alumina cement	63
Figure 4.10	Ball milled Ca(OH) <sub>2</sub> -CuO-TiO <sub>2</sub> mixtures	63
Figure 4.11	XRD patterns for stoichiometry Ca(OH) <sub>2</sub> -CuO-TiO <sub>2</sub> mixtures ball milled for 1 hour	64
Figure 4.12	(a) CaCu <sub>3</sub> Ti <sub>4</sub> O <sub>12</sub> powders after calcination process, (b) alumina crucible used during calcination stage	65
Figure 4.13	XRD pattern of calcined CaCu <sub>3</sub> Ti <sub>4</sub> O <sub>12</sub> at 750 °C for 12 hours	65
Figure 4.14	CaCu <sub>3</sub> Ti <sub>4</sub> O <sub>12</sub> green body (yellow) after compaction and CaCu <sub>3</sub> Ti <sub>4</sub> O <sub>12</sub> dense pellet (black) after sintering for 24 hours at 1000 °C	66
Figure 4.15	XRD pattern of sintered CaCu <sub>3</sub> Ti <sub>4</sub> O <sub>12</sub> pellet at 1000 °C for 24 hours	67
Figure 4.16	Dielectric constant and dissipation factor as a function of frequency for pellet sintered at 1000 °C for 24 hours	68
Figure 4.17	Calcined powders of Zr-doped CaCu <sub>3</sub> Ti <sub>4</sub> O <sub>12</sub> inside alumina crucible	69
Figure 4.18	Comparison of XRD patterns for 0.06 mole % Zr-doped CaCu <sub>3</sub> Ti <sub>4</sub> O <sub>12</sub> sintered pellet at 1000 °C for 24 hours and the standard sample	70

Figure 4.19	Relative density and porosity of sintered pellets prepared from furnace technique	71
Figure 4.20:	Dielectric properties as a function of composition for pellets sintered at 1000 °C for 24 hours	72
Figure 4.21	SEM micrograph of: Zr-doped $\text{CaCu}_3\text{Ti}_4\text{O}_{12}$ , (a) 0 mole % (b) 1 mole % and (c) 2 mole % sintered at 1000 ° for 24 hours	73
Figure 4.22	SEM micrograph of: Zr-doped $\text{CaCu}_3\text{Ti}_4\text{O}_{12}$ , (a) 4 mole % (b) 6 mole % and (c) 10 mole % sintered at 1000 ° for 24 hours	74
Figure 4.23	Average grain size of Zr-doped $\text{CaCu}_3\text{Ti}_4\text{O}_{12}$ sintered pellets	75
Figure 4.24	Calcination process for 30 minutes in microwave processing	76
Figure 4.25	Alumina crucible after heating in microwave oven for 5 minutes	76
Figure 4.26	Graphite crucible used as a susceptor in microwave processing	77
Figure 4.27	Comparison of XRD patterns of $\text{CaCu}_3\text{Ti}_4\text{O}_{12}$ calcined and sintered pellet in microwave oven using graphite crucible and the standard sample	78
Figure 4.28	SiC crucible used as a susceptor in microwave heating	79
Figure 4.29	Compacted pellet of $\text{CaCu}_3\text{Ti}_4\text{O}_{12}$ calcined for 30 minutes in microwave	80
Figure 4.30	XRD pattern of $\text{CaCu}_3\text{Ti}_4\text{O}_{12}$ calcined powders in microwave with different time, (a) standard $\text{CaCu}_3\text{Ti}_4\text{O}_{12}$ , (b) $\text{Ca}(\text{OH})_2$ - $\text{CuO}$ - $\text{TiO}_2$ mixtures after milling, (c) microwave heating for 30 minutes, (d) microwave heating for 60 minutes, (e) microwave heating for 90 minutes, (f) microwave heating for 120 minutes, (g) microwave heating for 150 minutes and (h) microwave heating for 30 minutes	86
Figure 4.31	SEM micrograph of $\text{CaCu}_3\text{Ti}_4\text{O}_{12}$ , calcined for (a) 30, (b) 60	87

	and (c) 90 minutes	
Figure 4.32	SEM micrograph of $\text{CaCu}_3\text{Ti}_4\text{O}_{12}$ , calcined for (a) 120, (b) 150 and (c) 180 minutes	88
Figure 4.33:	Average particle size of $\text{CaCu}_3\text{Ti}_4\text{O}_{12}$ calcined powder prepared from microwave heating technique	89
Figure 4.34	Particle size distributions of 12 hours calcination in furnace	90
Figure 4.35	Particle size distributions of 120 minutes calcination in microwave oven	90
Figure 4.36:	SEM micrograph of: (a) $\text{CaCu}_3\text{Ti}_4\text{O}_{12}$ sintered for 90 minutes and (b) $\text{CaCu}_3\text{Ti}_{3.99}\text{Zr}_{0.01}\text{O}_{12}$ sintered for 60 minutes using microwave	92

## LIST OF ABBREVIATION

$\text{CaCu}_3\text{Ti}_4\text{O}_{12}$	:	Calcium copper titanate
$\text{CaCu}_3\text{Ti}_{3.99}\text{Zr}_{0.01}\text{O}_{12}$	:	Calcium copper titanate with 0.01 mole fraction or 1 mole % of zirconium
$\text{CaCu}_3\text{Ti}_{3.98}\text{Zr}_{0.02}\text{O}_{12}$	:	Calcium copper titanate with 0.02 mole fraction or 2 mole % of zirconium
$\text{CaCu}_3\text{Ti}_{3.96}\text{Zr}_{0.04}\text{O}_{12}$	:	Calcium copper titanate with 0.04 mole fraction or 4 mole % of zirconium
$\text{CaCu}_3\text{Ti}_{3.96}\text{Zr}_{0.04}\text{O}_{12}$	:	Calcium copper titanate with 0.06 mole fraction or 6 mole % of zirconium
$\text{CaCu}_3\text{Ti}_{3.9}\text{Zr}_{0.1}\text{O}_{12}$	:	Calcium copper titanate with 0.1 mole fraction or 10 mole % of zirconium
FTIR		Fourier Transform Infrared
SEM	:	Scanning Electron Microscopy
XRD	:	X-ray diffraction

## LIST OF MAIN SYMBOL

%	Percentage
°	Degree
°C	Degree Celcius
°C/min	Degree Celcius per minutes
J	Joule
MPa	Mega Pascal
GPa	Giga Pascal
mg	milligram
g	Gram
nm	Nanometer
µm	Micrometer
mm	Milimeter
cm	Centimeter
m	Meter
wt %	Weight percent
λ	Wave length
s	second
min	minutes

## PEMROSESAN ELEKTROSERAMIK $\text{CaCu}_3\text{Ti}_4\text{O}_{12}$ BERDOP Zr DIBANTU

### GELOMBANG MIKRO

#### ABSTRAK

Penyediaan  $\text{CaCu}_3\text{Ti}_4\text{O}_{12}$  tulen dan yang didop dengan  $\text{ZrO}_2$  telah disediakan dengan kaedah tindak balas keadaan pepejal dan pemprosesan gelombang mikro. Bahan mentah  $\text{Ca(OH)}_2$ ,  $\text{CuO}$ ,  $\text{TiO}_2$  dan  $\text{ZrO}_2$  telah dikisar, dikalsin, dibentuk dan akhirnya disinter. Untuk menghasilkan  $\text{CaCu}_3\text{Ti}_4\text{O}_{12}$  tulen dan terdop, suhu pengkalsinan  $750\text{ }^\circ\text{C}$  dengan tempoh rendaman selama 12 jam telah dipilih untuk pembentukan sebatian  $\text{CaCu}_3\text{Ti}_4\text{O}_{12}$  manakala suhu persinteran adalah  $1000\text{ }^\circ\text{C}$  selama 24 jam. Komposisi pendopan pula telah divariasikan dari 1 hingga 10 molar %. Pemprosesan gelombang mikro telah dijalankan menggunakan ketuhar gelombang mikro. Hasil kajian XRD menunjukkan bahawa mangkuk pijar yang digunakan sebagai pemanas sangat mempengaruhi pembentukan fasa  $\text{CaCu}_3\text{Ti}_4\text{O}_{12}$ . Penggunaan alumina atau grafit tidak dapat menghasilkan sebatian  $\text{CaCu}_3\text{Ti}_4\text{O}_{12}$  yang sempurna. Oleh itu kajian telah diteruskan dengan menggunakan mangkuk pijar lain dan didapati bahawa 40 % berat partikel kasar silikon karbida tertabur di dalam simen alumina yang berfungsi sebagai pemanas adalah berkesan. Pengkalsinan selama 30 minit menggunakan gelombang mikro telah dapat menghasilkan fasa tunggal  $\text{CaCu}_3\text{Ti}_4\text{O}_{12}$ . Persinteran selama 90 minit didapati telah dapat menghasilkan pelet  $\text{CaCu}_3\text{Ti}_4\text{O}_{12}$  yang tumpat. Pemalar dielektrik  $\text{CaCu}_3\text{Ti}_4\text{O}_{12}$  yang dihasilkan melalui kaedah lazim lebih tinggi berbanding kaedah gelombang mikro. Walau bagaimanapun, nilai lesapan dielektrik yang dihasilkan daripada kaedah gelombang mikro adalah lebih rendah.

**MICROWAVE ASSISTED PROCESSING OF Zr-DOPED  $\text{CaCu}_3\text{Ti}_4\text{O}_{12}$   
ELECTROCERAMICS**

**ABSTRACT**

Preparation of pure  $\text{CaCu}_3\text{Ti}_4\text{O}_{12}$  and  $\text{ZrO}_2$  doped  $\text{CaCu}_3\text{Ti}_4\text{O}_{12}$  have by been done by solid state reaction and microwave processing. Starting materials,  $\text{Ca}(\text{OH})_2$ ,  $\text{CuO}$ ,  $\text{TiO}_2$  and  $\text{ZrO}_2$  are subsequently milled, calcined, compacted and sintered. To produce pure  $\text{CaCu}_3\text{Ti}_4\text{O}_{12}$  and  $\text{ZrO}_2$  doped  $\text{CaCu}_3\text{Ti}_4\text{O}_{12}$ , the calcination temperature is  $750^\circ\text{C}$  with 12 hours soaking time in the furnace whereas the sintering process has been done at  $1000^\circ\text{C}$  with 24 hours soaking time. Dopant composition had been verified from 1 until 10 mole %. Microwave processing has been done by microwave oven. Based on phase analysis using XRD, the crucible used as susceptor is important in order to produce single phase  $\text{CaCu}_3\text{Ti}_4\text{O}_{12}$ . Alumina and graphite had been used as a crucible but the calcination is not completed. Research continued with another crucible and single phase  $\text{CaCu}_3\text{Ti}_4\text{O}_{12}$  had been successfully synthesized at calcinations time of 30 minutes in microwave oven using 40 wt.% coarse silicon carbide particles distributed in an alumina cement matrix as a susceptor. Sintering for 90 minutes in microwave oven has produced dense pellet of  $\text{CaCu}_3\text{Ti}_4\text{O}_{12}$ . The dielectric constant of pellet derived from different processing had been compared and it was found that  $\text{CaCu}_3\text{Ti}_4\text{O}_{12}$  from furnace heating shows higher value than microwave processing. The dissipation factor of pellet from microwave processing showed lower value than pellet from furnace heating.



# CHAPTER 1

## INTRODUCTION

### 1.1 Ceramic Materials

Ceramic materials are compounds between metallic and nonmetallic, mostly are oxides, nitrides and carbides. Ceramics are composed of clay minerals, cement and glass. These materials are insulator because of its properties that are insulative to the passage of electricity and heat. Ceramics are more resistant in high temperatures and harsh environment than metal and polymers. Ceramics are known as Keramos, means of pottery or white wares that made from clays and will go through firing process. Pottery is based on clay and other siliceous minerals. The clays have special property that on mixing with water they form a mouldable paste. Articles made from this paste remain in the shape it was while wet, on drying and on firing. This firing process involves high temperature, between 800-1200 °C temperature ranges. The temperature used in firing process of ceramics materials is depending on the product that will be produced. The production of white wares needs temperature between 800 °C to 1100 °C. White porcelain production needed high temperature, 1200 °C to 1400 °C (Kingery, 1976). Pottery is chemically stable after firing so it can be used to store water and food. It can sustain in normal usage although its brittleness renders it susceptible to mechanical and thermal shock.

The evolution from pottery to advanced ceramics has expanded the explanation of the word 'ceramics' so that it now means a solid article which has as its important component, and is composed in large part of inorganic non-metallic materials. This term is only limited to polycrystalline, inorganic, non-metallic materials that get their mechanical strength through firing or sintering process.

The first application of ceramics materials in electronic industry is based on the nature properties of ceramics, which are high electrical resistance and their stability when exposed to extremes of environments like high temperature. The obvious characteristic of ceramics in the first half of the twentieth century was about chemical stability and high resistivity. The development from year 1910 onwards of electronics materials shows many ceramics substance have been synthesized. Nickel-zinc and manganese zinc ferrites, closely allied in structure to magnetite, were used as choke and transformer core materials for applications at frequencies up to and beyond 1 MHz because of their high resistivity and consequently low susceptibility to eddy currents. From 1940 onwards magnetic ceramic powders form the basis of recording tapes (Moulson and Herbert, 2003).

Ceramic materials serve important insulative, capacitive, conductive, resistive, sensor, electrooptic and magnetic functions in a wide variety of electrical and electronic circuitry. Traditional voltage insulative uses have involved mainly dielectric isolation of conductors and various active devices. Glass insulators, ceramic heater substrates for microelectronics packaging, are all primary used in this mode.

The term electroceramics are used to explain ceramics materials that have been formulated for electrical, magnetic or optical properties. These properties can be change in order to the ceramics materials work as capacitor with high dielectric constant, ferroelectric materials, ferrites for data and information storage, high conductive ceramics or sensor.

The development in various subclasses of electroceramics has parallel with new technologies. Electroceramics materials that have high dielectric constant can be used for construction of ceramic capacitor. Dielectric materials have high electrical resistance but support the electric field efficiently. Lowering the dielectric loss will increase the efficiency

of dielectric materials. Ceramics as dielectrics for capacitors have the disadvantage because it is difficult to prepare as self-supporting thin plates and, if this is achieved, are extremely fragile. However, the introduction of titania ( $\epsilon_r \approx 100$ ) led to the development of capacitors having values in the 1000 pF range in convenient sizes but with a high negative temperature coefficient and gives very stable units (Moulson and Herbert, 2003).

Dielectric materials are insulator used for their exceptional dielectric properties. When a material is introduced between two plates of capacitor, the total charge stored in the capacitor will change. The change depends on the ability of the material to polarize under an electric field. The dielectric constant or permittivity determines the change in charge storage. For high capacity application, a high dielectric constant is needed.

Materials with high dielectric constants are widely used in technological applications such as capacitors, resonators and filters. High dielectric constants allow smaller capacitive components, thus offering the opportunity to decrease the size of electronic devices. Capacitors are essential components of most electronics circuit because these devices can store electrical energy.

## **1.2 Problem Statement**

The quality of ceramic products depends on time and the temperature at which they are fired. Firing of ceramic materials always is carried out by placing these materials in furnace. The mechanism of furnace heating methods is heat conduction from the material's surface inward, thus generate temperature gradient between outer and inner surface of the heated material. Furnace heating methods overcure the surface while undercuring the interior. Furnace heating is slow and inefficient for materials that conduct heat poorly. Furnace parameters that must be controlled include temperature, pressure,

heating and cooling rates and atmosphere condition. High temperatures are required to achieve the desired strength and composition. During firing process, the material is soaked for few hours to get the desirable properties. The high temperature and longer time in conventional heating will increase the production cost. In order to retain or reduce the cost, microwave energy (microwave frequency) is being developed as a new tool for high temperature processing of materials.

Very recently, microwave heating technique has been successfully devised to synthesized electroceramics. Although only a few electroceramics have been synthesized by microwave heating, it should not be overlooked as a reliable synthesis method. Microwave heating is a quick and efficient method of heating materials that are difficult to heat by convection or infrared methods because the type of heating is volumetric heating, so production rates increase and product quality improves. Microwave heating is an electromagnetic spectrum with a frequency between 300 MHz to 300 GHz. Microwave heating have several properties as same as visible light that are may be reflected or absorbed by the material, may transmit through materials without any absorption and when traveling from one material to another, the microwaves may change direction. The radiation of microwave is non-ionizing and different from the ionizing radiation such as x-rays and gamma rays. Materials absorb microwave energy through relaxation mechanism like dipolar, ion jump and ohmic loses. Two important parameters for microwave processing are power absorbed ( $P$ ) and depth of microwave penetration ( $D$ ). Unlike conventional heating, these parameters are highly dependent on the dielectric properties of the material and, in practice, can provide another degree of process flexibility. The factor to consider in microwave heating is the susceptor. Examples of the advantages associated with microwave processing are rapid and uniform heating, decreased sintering temperatures and reduce the long soaking time in conventional heating.

### 1.3 Research Objective

This study is focus on the comparison of  $\text{CaCu}_3\text{Ti}_4\text{O}_{12}$  doped by  $\text{ZrO}_2$  synthesise via furnace and microwave oven, the calcination time and sintering duration for microwave heating. Therefore, the objectives are:

- I. To synthesise  $\text{ZrO}_2$ -doped  $\text{CaCu}_3\text{Ti}_4\text{O}_{12}$  by conventional and microwave oven processing from starting materials of  $\text{Ca(OH)}_2$ ,  $\text{CuO}$ ,  $\text{TiO}_2$  and  $\text{Zr}_2\text{O}_3$
- II. To investigate the structures, morphology, electrical and dielectric properties of prepared samples.
- III. To compare the properties of  $\text{ZrO}_2$ -doped  $\text{CaCu}_3\text{Ti}_4\text{O}_{12}$  derived from microwave oven and conventional processing.

## **CHAPTER 2**

### **LITERATURE REVIEW**

#### **2.1 Introduction**

Electroceramics are ceramic materials that are specially formulated for special electrical, magnetic or optical circuit applications. The subclasses of electroceramics can be categorized according to their properties, which are piezoelectric, pyroelectric and ferroelectric (as one group), semiconductor, electro-optic ceramics, magnetic ceramics and ceramic superconductors. The ceramic properties which are important for electronic applications result from a variety of mechanism which depends on the bulk material, grain boundary properties and surface effects. Important properties include dielectric constant, dielectric strength, electrical conductivity, dielectric tangent and power loss.

#### **2.2 Dielectric Materials**

Dielectric materials are materials that have the basic electric properties of being polarized in the presence of electric field and having an electrostatic field within them under the state of polarization. They are insulator because the energy gap between the valence and conduction band is large. Dielectric materials do not conduct current but in the presence of electric field it can form an electrical dipole. The field may cause a slight shift in the balance of charge within the material to form an electrical dipole. Therefore, these materials are called “dielectric” materials. The dielectric materials can be of bulk, thick film or thin film form.

#### **2.3 Dielectric Properties**

Dielectric constant and dissipation factor are some of the most common measurement used to characterize a capacitor. Dielectrics and insulators can be defined

as materials with high electrical resistivities. Dielectrics fulfill circuit functions for which their permittivity  $\epsilon$  and dissipation factors,  $\tan \delta$  are also of primary importance. Insulators are used principally to hold conductive elements in position and to prevent them from coming in contact with one another. A good dielectric is necessarily a good insulator.

Dielectric is a term given to an electrically insulating material. Dielectric constant is the factor by which the capacitance of a parallel-plate capacitor is increased by inserting a dielectric in place of a vacuum. Insulators are materials with low conductivity. This low conductivity of roughly 20 orders of magnitude (compared with typical metals) is the result of energy band gaps greater than 2 eV (compared to zero for metals). These low conductivity materials are an important part of the electronics industry (Shackelford, 1996). The small degree of conductivity for insulators is not the result of thermal promotion of electrons across the band gap. Instead, it may be due to electrons associated with impurities in the materials. It can also result from ionic transport.

A dielectric material is one that is electrically insulating (nonmetallic) and exhibits or may be made to exhibit an electric dipole structure. The electric dipole structure is a separation of positive and negative electrically charged entities on a molecular or atomic level. As a result of dipole interactions with electric fields, dielectric materials are utilized in capacitors.

When a voltage is applied across a capacitor, one plate becomes positively charged, the other negatively charged, with the corresponding electric field directed from the positive to the negative. The capacitance,  $C$  is related to the quantity of charge stored on either plate,  $Q$  by

$$C = \frac{Q}{V} \quad (\text{Equation 2.1})$$

where  $V$  is the voltage applied across the capacitor. The units of capacitance are coulombs per volts, or farads (F). If we consider a parallel capacitor with a vacuum in the region between the plates as shown in Figure 2.1a, the capacitance can be computed from

$$C = \epsilon_0 \frac{A}{l} \quad (\text{Equation 2.2})$$

where  $A$  represents the area of the plates and  $l$  is the distance between them. The parameter  $\epsilon_0$ , called the permittivity of a vacuum, is a universal constant having the value of  $8.85 \times 10^{-12}$  F/m. If the dielectric material is inserted into the region within the plates as shown in Figure 2.1b, then

$$C = \epsilon \frac{A}{l} \quad (\text{Equation 2.3})$$

where  $\epsilon$  is the permittivity of this dielectric medium, which will be greater in magnitude than  $\epsilon_0$ . The relative permittivity  $\epsilon_r$ , often called the dielectric constant, is equal to the ratio

$$\epsilon_r = \frac{\epsilon}{\epsilon_0} \quad (\text{Equation 2.4})$$

The value is greater than unity and represents the increase in charge storing capacity by insertion of the dielectric medium between the plates. The dielectric constant is one material property that is of major consideration for capacitor design (Callister, 2000).

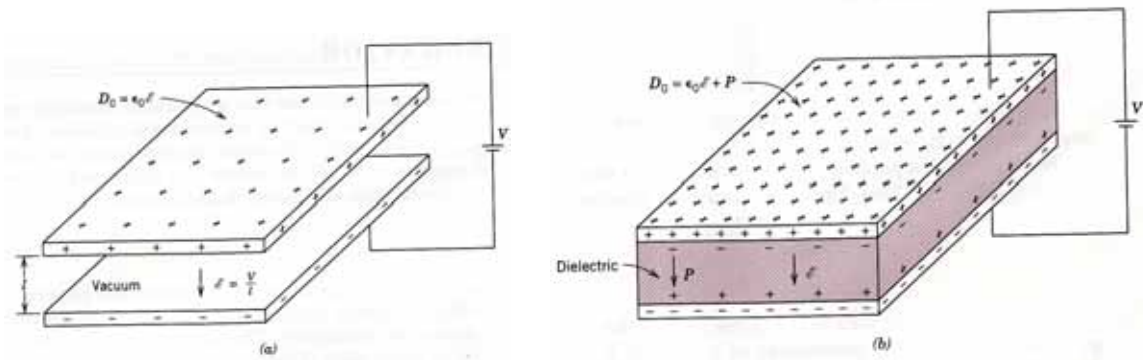


Figure 2.1: A parallel-plate capacitor (a) when a vacuum is present and (b) when a dielectric material is present (Callister, 2000)

The inserted dielectric material has increased the capacity by the factor of  $\epsilon_r$ . Table 2.1 lists the dielectric constant value for some dielectric materials at room temperature (Kahn, *et. al.*, 1988).

Table 2.1: Dielectric Constant at 25 °C

Material	Dielectric Constant
Teflon	2.1
Silica glass	3.8
PVC	4.6
Al <sub>2</sub> O <sub>3</sub>	9.9
MgTiO <sub>3</sub>	2
TiO <sub>2</sub>	100
CaTiO <sub>3</sub>	160
SrTiO <sub>3</sub>	320
BaTiO <sub>3</sub>	1000-2000

In the ceramic dielectric, losses will occur and specified by the dissipation factor, loss angle or loss tangent ( $\tan \delta$ ). The dissipation factor is a measure of capacitor efficiency that represents the relative expenditure of energy to obtain a given amount of charge storage (Hench and West, 1990). Dielectric loss is the result of continually reversing the polarity of electric field through the dielectric material; each time the molecular structure of the dielectric materials has to adjust a new polarity, a little electric energy will be converted into heat energy (Fowler, 1994). The dissipation factor is also influenced by a few mechanisms such as ion migration, ion vibration and ion deformation and all of these things are strongly affected by the temperature and frequency (Gao and Sammes, 1999).

## 2.4 Perovskite Structure

Perovskite was discovered in the Ural mountains of Russia by Gustav Rose in 1839 and named for Russian mineralogist, L. A. Perovski. This name perovskite has been later used for the designation of a large  $ABO_3$  perovskite family. Perovskite structure is adopted by many oxides that have the chemical formula  $ABO_3$ . The structure is very versatile having many useful technological applications such as ferroelectrics, catalysts, sensors and superconductors (Lemanov, *et. al.*, 1999). The generalized perovskite structure  $ABO_3$  is visualized as based on a cubic close-packed assembly. Homes, *et. al.*, (2001) mentioned the perovskite-related body centered cubic (bcc) of  $CaCu_3Ti_4O_{12}$  structure is a combination of  $Ca^{2+}$  cation in the A site,  $Cu^{2+}$  cation in the B site while  $O_3$  is occupied by oxygen as shown in Figure 2.2. In the figure, several unit cells of  $CaCu_3Ti_4O_{12}$ , shown as  $TiO_6$  octahedra. Each of the atom was differentiated by different color.

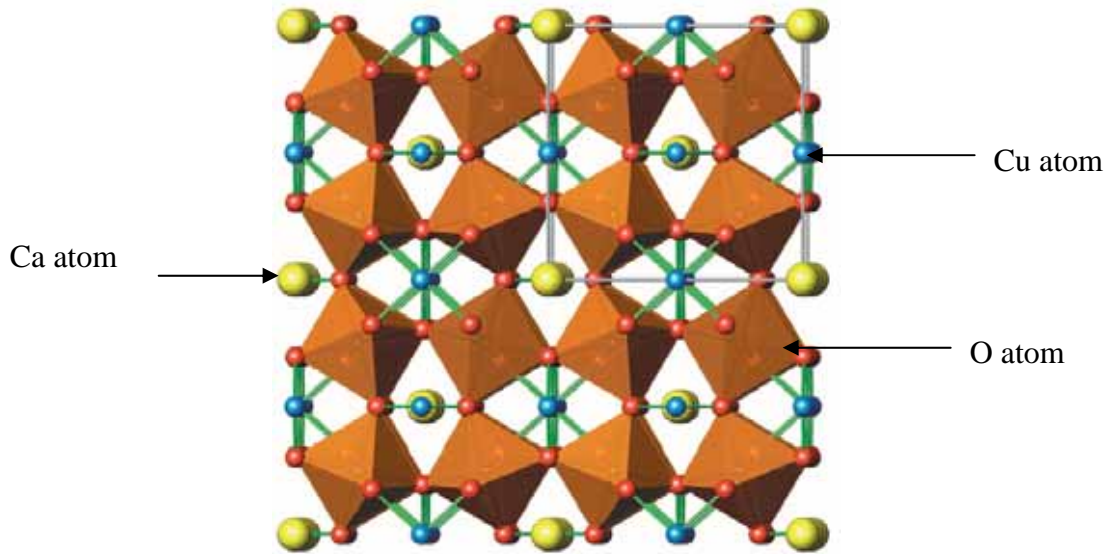


Figure 2.2: Several unit cells of  $\text{CaCu}_3\text{Ti}_4\text{O}_{12}$ , shown as  $\text{TiO}_6$  octahedra, Cu atoms (blue) bonded to four oxygen atoms (red), and large Ca atoms (yellow) without bonds (Homes, *et. al.*, 2001)

The general crystal structure is a primitive cube, with the A-cation in the middle of the cube, the B-cation in the corner and the anion, commonly oxygen, in the centre of the face edges. The structure is stabilized by the 6 coordination of the B-cation (octahedron) and 12 of the A cation. The packing of the ions can be thought of the A and O ions together form a cubic close packed array, where the B ions occupy a quarter of the octahedral holes. Subramanian, *et. al.*, (2003) cited that the space for the A cations is essentially fixed, and the twelve equal A–O distances must be very close to 2.6 Å for  $\text{CaCu}_3\text{Ti}_4\text{O}_{12}$  perovskite structure. Perovskites possess high values for  $\epsilon_0$  and are widely used in such technological applications. Another type of perovskite that is widely study is barium titanate ( $\text{BaTiO}_3$ ) having both  $\text{Ba}^{2+}$  and  $\text{Ti}^{4+}$  cations. The  $\text{Ba}^{2+}$  ions are located at the corners of the unit cell, which is of tetragonal symmetry (a cube that has been elongated slightly in one direction). The dipole moment results from the relative

displacement of the  $O^{2-}$  and  $Ti^{4+}$  ions from their symmetrical positions. When barium titanate is heated above its ferroelectric Curie temperature (120 °C), the crystal structure become cubic and all ion assumed symmetric positions within the cubic unit cell.

## 2.5 $CaCu_3Ti_4O_{12}$

$CaCu_3Ti_4O_{12}$  is a result obtained by reaction of three raw materials,  $CaCO_3$ ,  $CuO$  and  $TiO_2$ . A review by Jin, *et. al.*, (2007) has singed that  $CaCu_3Ti_4O_{12}$  was generally prepared by the traditional solid-state method.

The starting materials were weighed according to the stoichiometric ratio (Jha, *et. al.*, 2003). The mixing process can be done either by agate mortar or conventional ball milling. The mixed powder was calcined at temperature ranging from 750-950 °C for 12 hours. The calcined powder was pressed into pellet shape with diameter ranging from 5-16 mm. The pellets were sintered in air at temperature ranging from 1000-1050 °C for 20-24 hours. The ramping and cooling rate for both calcinations and sintering was 5 °C/m.

$CaCu_3Ti_4O_{12}$  shows a dielectric constant at 1 kHz of about 12,000 that is nearly constant from room temperature to 300 °C. The cubic structure of these materials is related to that of perovskite ( $CaTiO_3$ ), but the  $TiO_6$  octahedra are tilted to produce a square planar environment for  $Cu^{2+}$ . The structure remains cubic and centric. Most compositions of the type  $A_{2/3}Cu_3Ti_4O_{12}$  ( $A$  = trivalent rare earth or Bi) show dielectric constants above 1000 (Subramanian, *et. al.*, 2000).

The  $ACu_3Ti_4O_{12}$  family of compounds has been known since 1967 and accurate structures as shown in Figure 2.1 were determined in 1979. Figure 2.3 showed the structure of  $CaCu_3Ti_4O_{12}$  which consists of two formula units. Ti atoms sit at the center of

the canted  $\text{TiO}_6$  octahedra (the tilt angle is nominally  $141^\circ$ ), with bridging Cu atoms bonded to the oxygen atoms, and large Ca atoms at the corners and center of the unit cell. The copper atoms bonded to four oxygen atoms, and large calcium atoms without bonds.

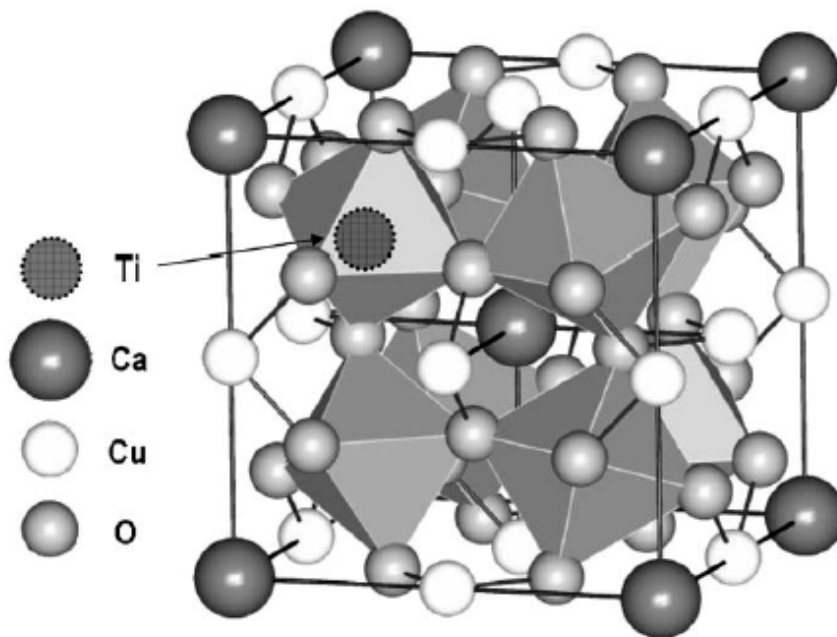


Figure 2.3: Unit cell of body-centered cubic  $\text{CaCu}_3\text{Ti}_4\text{O}_{12}$  in the  $\text{Im}\bar{3}$  space group (Manik *et. al.*, 2006).

Apparently, the dielectric properties of these compounds have not been previously examined. Dielectric constant is the ratio of the permittivity of a medium to that of a vacuum, often called the relative dielectric constant or relative permittivity. The dielectric constant and loss component ( $\tan \delta$ ) for two different samples of  $\text{CaCu}_3\text{Ti}_4\text{O}_{12}$  are shown as a function of temperature at a frequency of 1 kHz, in Figure 2.4. The dielectric constant for  $\text{CaCu}_3\text{Ti}_4\text{O}_{12}$  decreases with increasing frequency, to a value of 9200 at 1MHz (Ramirez, *et. al.*, 2000). This is because the dipole charge cannot move when polarization rate of electric field increased.

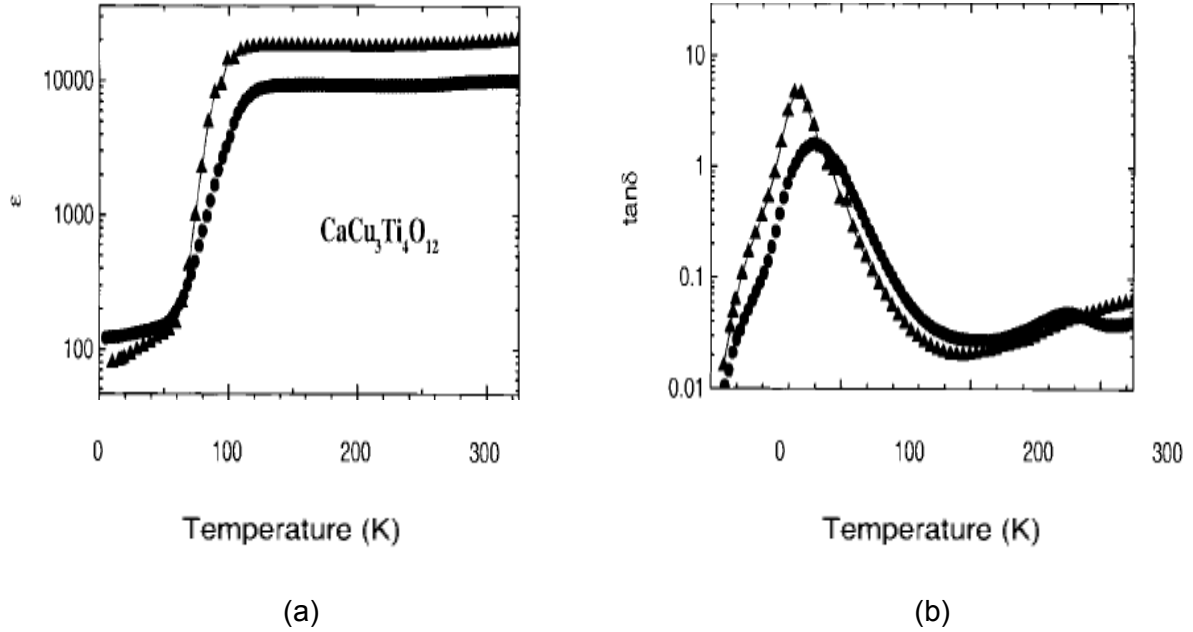


Figure 2.4: (a) The real part of the dielectric constant,  $\epsilon$  (T), for two different samples of  $\text{CaCu}_3\text{Ti}_4\text{O}_{12}$ . (b) The loss component of the dielectric response, expressed as  $\tan \delta$  (Ramirez, *et. al.*, 2000).

The dielectric properties of  $\text{CaCu}_3\text{Ti}_4\text{O}_{12}$  are depending on the grain boundary, the presence of twin boundaries, planar defects and displacements of Ti ions.  $\text{CaCu}_3\text{Ti}_4\text{O}_{12}$  has a large value of dielectric constant ( $\epsilon'$ ). The dielectric constant value for  $\text{CaCu}_3\text{Ti}_4\text{O}_{12}$  exhibits only small variations with changes in temperature and frequency. These properties are desirable for technological applications. Based on the previous research, the cause of high permittivity in  $\text{CaCu}_3\text{Ti}_4\text{O}_{12}$  are due to intrinsic mechanism and extrinsic mechanism. The giant dielectric is measured in a perfectly stoichiometry, defect free and single domain crystal of  $\text{CaCu}_3\text{Ti}_4\text{O}_{12}$  in intrinsic mechanism. In extrinsic mechanism, the giant dielectric response is associated with defects, domain boundaries or other crystalline deficiencies.

### 2.5.1 Grains boundaries effect

Grain boundaries play a major role in the dielectric properties of  $\text{CaCu}_3\text{Ti}_4\text{O}_{12}$  (Zang, *et. al.*, 2005). When an impedance spectroscopy analysis done on  $\text{CaCu}_3\text{Ti}_4\text{O}_{12}$  ceramics, the data shown that they are electrically heterogeneous and consist of semiconducting grains with insulating grain boundaries. Sinclair, *et. al.*, (2005) suggested that the giant dielectric response is due to a grain boundary (internal) barrier layer capacitance (IBLC). Figure 2.5a shows the variations of dielectric dispersion within a frequency range of 100 Hz to 100 kHz. The three different  $\text{CaCu}_3\text{Ti}_4\text{O}_{12}$  ceramic samples were sintered for 10, 20 and 80 hours respectively. The sample that has been sintered for 80 hours showed a value of the dielectric constant greater than 60 000 when measured at room temperature. From this figure, we can see at 100 kHz, each of the dielectric curves shows a sharp decrease and this situation happened again at frequencies higher than 6 MHz. Figure 2.5b shows a good linear relationship between  $\ln(J/AT^2)$  versus  $E^{1/2}$  obtained for each sample. These relationships demonstrated the presence of Schottky barrier at the grain boundary.

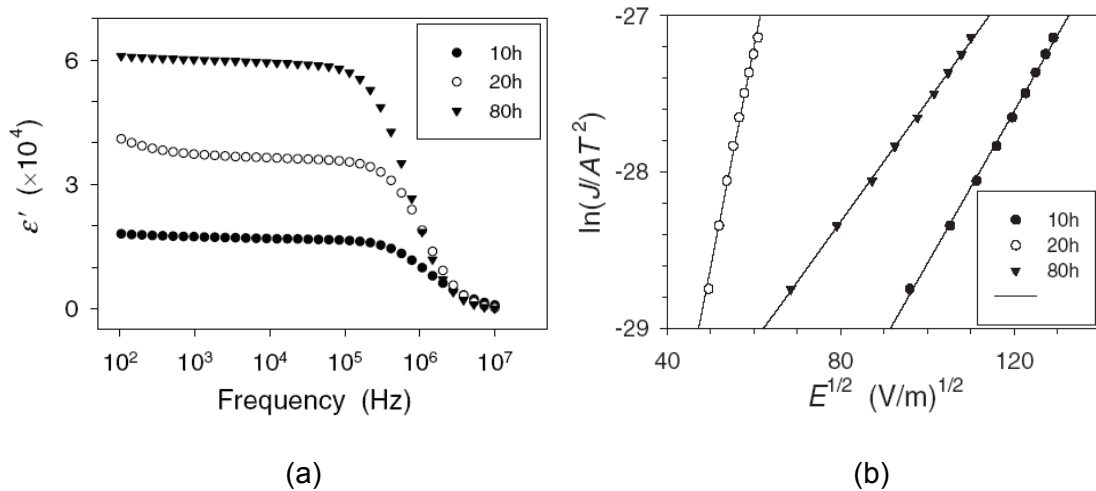


Figure 2.5: (a) The real part,  $\epsilon'$ , of the dielectric dispersion at different frequency and (b) plots of  $\ln(J/AT^2)$  versus  $E^{1/2}$  of three different  $\text{CaCu}_3\text{Ti}_4\text{O}_{12}$  ceramic samples measured at room temperature (Zang, *et. al.*, 2005).

Figure 2.6 showed the Scanning Electron Microscope (SEM) photographs of the ceramic samples, sintered for 20 and 80 hours. The grain size was obtained using the interception method. Sample with a longer sintering time exhibits a larger dielectric constant. Accordingly, the sample with a longer sintering time has the larger grain size.

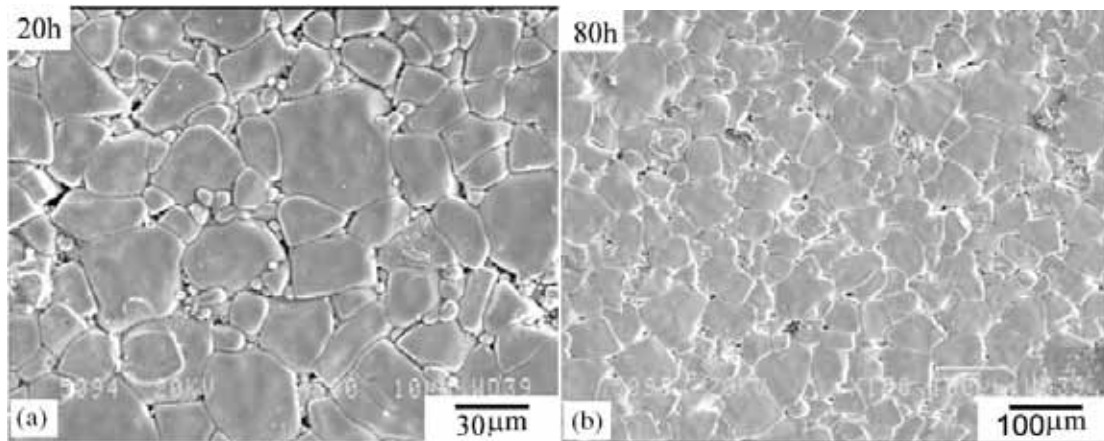


Figure 2.6: SEM photographs of the two  $\text{CaCu}_3\text{Ti}_4\text{O}_{12}$  ceramic samples which were sintered for 20 hours and 80 hours (Zang, *et. al.*, 2005).

### 2.5.2 Processing effect

The extrinsic mechanism most commonly believed to be the source of  $\text{CaCu}_3\text{Ti}_4\text{O}_{12}$  high permittivity is the formation of internal capacitive barrier layers (Subramanian, *et. al.*, 2000). It is believed that during processing of  $\text{CaCu}_3\text{Ti}_4\text{O}_{12}$  that insulating surfaces form on semiconducting grains creating an electronically heterogeneous material very similar in nature to internal barrier layer capacitors (IBLC). The dielectric properties of these materials are very sensitive to different processing parameters. Mixing technique, calcinations temperature, sintering temperature, time of sintering and argon annealing will affect the dielectric properties of  $\text{CaCu}_3\text{Ti}_4\text{O}_{12}$  (Bender, *et. al.*, 2005).

$\text{CaCu}_3\text{Ti}_4\text{O}_{12}$  was prepared using mortar and pestle, known as conventional ceramic solid state reaction processing techniques and the value of room temperature permittivity was 11,700 with 0.047 dielectric losses. When  $\text{CaCu}_3\text{Ti}_4\text{O}_{12}$  powder prepared using attrition mill, the permittivities value was close to 100,000. Sintering temperature for  $\text{CaCu}_3\text{Ti}_4\text{O}_{12}$  also affect the dielectric constant value. At the sintering temperature increased from 990 to 1050 °C, both the dielectric constant (714 to 82,450) and loss (0.014 to 0.98) enhanced (Bender, *et. al.*, 2004).

Different time of sintering also led to change in permittivity, which longer sintering time will have higher dielectric constant. Figure 2.7 shows the dielectric dispersion at 225 K of  $\text{CaCu}_3\text{Ti}_4\text{O}_{12}$  sintered at 1100 °C for 2.5, 5, 7.5, 10 and 15 hours. Increasing the sintering duration enhanced the dielectric constant and it remains nearly constant till 100 kHz for the entire sample before drops to lower value that is below 100. The dielectric constant for the sample sintered at 1100 °C for 2.5 hour is only 2400 at 10 kHz.

When the sintering duration was increased to 5 hour, the dielectric constant improved to 13,000 at 10 kHz. Prakash, *et. al.*, (2006) described this situation because of the remarkable change in the microstructure in which some grains show abnormal growth and Cu-rich smaller grains occupying the intermittent regions. Further increase in the sintering duration to 15 hour increased the dielectric constant to more than 24,000. Density differences and grain size were not having a strong effect to improve the dielectric constant. When  $\text{CaCu}_3\text{Ti}_4\text{O}_{12}$  sample annealed in flowing argon at 1000 °C, the dielectric constant was close to one million at room temperature.

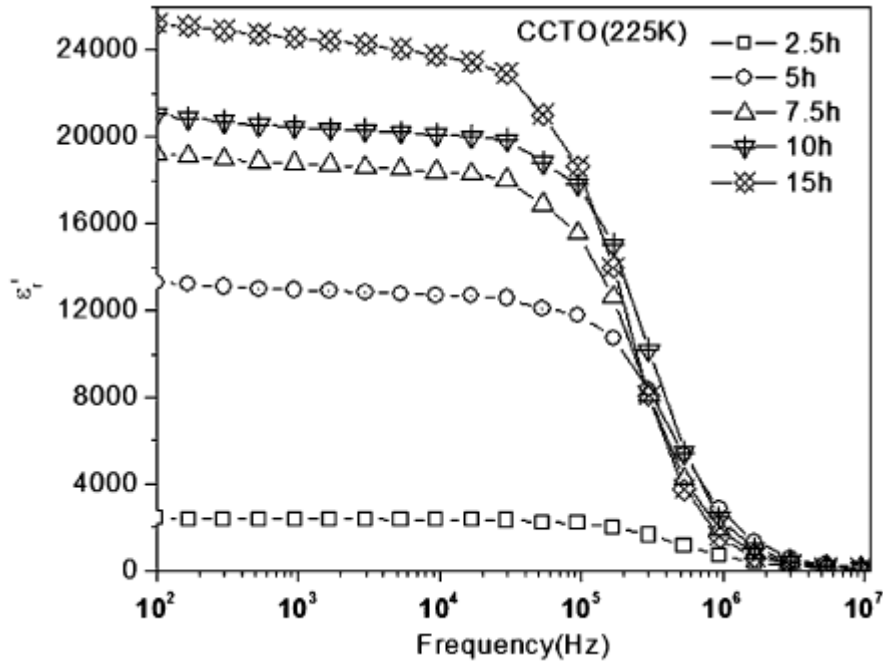


Figure 2.7: Frequency dependence of real part of dielectric constant ( $\epsilon_r'$ ) at 225 K for  $\text{CaCu}_3\text{Ti}_4\text{O}_{12}$  pellets sintered for different durations at 1100 °C [Prakash, *et. al.*, 2006].

### 2.5.3 Electrode/sample contact effects

The high dielectric constant in  $\text{CaCu}_3\text{Ti}_4\text{O}_{12}$  is related to the ceramic itself and from the electrode/sample contact effects which depends on the surface resistivity of the sample. There will be no mobile space charges when the surface resistivity is as high as  $1.2 \times 10^8 \Omega$  so the dielectric properties of the sample is inert to the different metal electrodes and various sample thickness. Under this condition, the dielectric constant is near 2000 at frequency equal to 10 kHz at room temperature, due to the true properties of ceramic (Yang, *et. al.*, 2005). When the surface resistivity was decreased to  $3.1 \times 10^7 \Omega$  via post annealing the sample in  $\text{N}_2$  atmosphere at 750 °C, the dielectric sample become sensitive to the different types of contact because space charges can be observed. Measurement of the dielectric constant of the sample using platinum (Pt) electrode shows a significant change when the dielectric constant increased to 5000 at 10 kHz compared to

argentums (Ag) electrode. Figure 2.8a shows the frequency dependence of the dielectric constant at room temperature for the  $\text{CaCu}_3\text{Ti}_4\text{O}_{12}$  ceramic coated with various metal electrodes. There are slight changes for the dielectric constant of the sample with different contacts in the frequency region of 100 Hz and 1 MHz. From the figure, the dielectric constant for silver paint and evaporated silver are quit same. This result indicated that the dielectric constant of the sample is inert to the different types of contacts. Lunkenheimer, *et. al.*, (2004) stated that the dielectric properties of  $\text{CaCu}_3\text{Ti}_4\text{O}_{12}$  is sensitive to metal contact because the high dielectric constant exhibit by this material is due to the formation of the Schottky barriers between the electrodes and the sample. In order to reduce the resistivity of the sample to form the Schottky barriers, the samples were annealed. Figure 2.8b shows the dielectric constant of  $\text{CaCu}_3\text{Ti}_4\text{O}_{12}$  sample become sensitive to the different contacts.

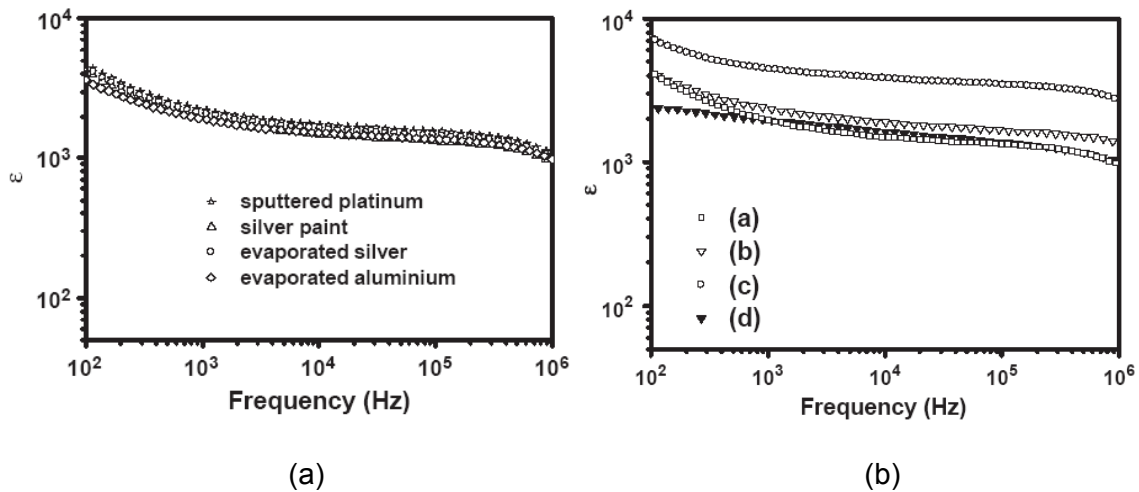


Figure 2.8: (a) Frequency dependence of the dielectric constant at room temperature for  $\text{CaCu}_3\text{Ti}_4\text{O}_{12}$  sample with different electrodes, (b) Dielectric constant at room temperature for sample (a) with silver paint electrode, (b) annealed in  $\text{N}_2$  at  $750^\circ\text{C}$  for 8 h with silver paint electrode, (c) annealed in  $\text{N}_2$  at  $750^\circ\text{C}$  for 8 h with the Pt electrode, (d) annealed in  $\text{O}_2$  at  $750^\circ\text{C}$  for 16 h with Pt electrode (Yang, *et. al.*, 2005)

#### 2.5.4 Chemical Modifications on $\text{CaCu}_3\text{Ti}_4\text{O}_{12}$

The dielectric properties, electrical conduction and the internal domains of  $\text{CaCu}_3\text{Ti}_4\text{O}_{12}$  ceramics are dependant to the substitution of other ions for copper ions ( $\text{Cu}^{2+}$ ) or titanium ions ( $\text{Ti}^{4+}$ ) (Fang, *et. al.*, 2006). During powder processing, dopants are usually added to improve densification, in terms of increasing the packing density of powder compacts. Dopants are often used to enhance the material transport rate during sintering by increasing the lattice diffusivity. Dopants can also be used to prevent exaggerated grain growth and to permit a complete densification with minimal porosity entrapment.

##### 2.5.4.1 Isovalent Substitution

The ions of  $\text{CaCu}_3\text{Ti}_4\text{O}_{12}$  perovskite structure can be substituted by an ion with similar size and charge.  $\text{Ti}^{4+}$  can be replaced by ions such as zirconium ( $\text{Zr}^{4+}$ ) and silicon ( $\text{Si}^{4+}$ ). The primary source of zirconia is the mineral zircon ( $\text{ZrO}_2 \cdot \text{SiO}_2$ ). Zirconia is normally act as a stabilizer or partially stabilized product for use in high temperature applications so that the effects of the phase transition at 1100 °C from monolithic to cubic or tetragonal is negated. A study on other system like  $\text{BaTiO}_3$  showed that Zr-doped  $\text{BaTiO}_3$  solid solution resulted with highest values of dielectric constant are almost at the same temperature, it is around 130 °C. Figure 2.9 shows the dielectric constant versus temperature of  $\text{BaTiO}_3$  ceramics with different concentration of  $\text{Zr}^{4+}$ . This figure shows that the dielectric properties of Zr-doped  $\text{BaTiO}_3$  are not highly affected by the amount of  $\text{Zr}^{4+}$  ions (Lee, *et. al.*, 1995).

Dopants are usually oxides of metals that have valences different from the primary oxide. These oxides are soluble in the primary oxide and added primarily for their effects on the electronics and ionic transport properties of the primary oxide.

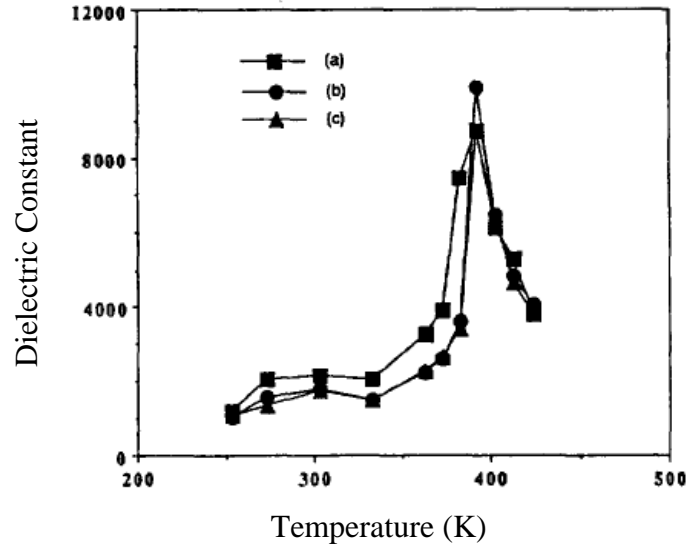


Figure 2.9: The dielectric constants versus temperature of Zr-doped BaTiO<sub>3</sub> ceramics (a) with 0.8 at.% (b) with 2 at.% and (c) with 5 at.% (frequency = 1 kHz) (Lee, *et. al.*, 1995).

Figure 2.10 shows the surface from scanning electron microscope micrographs of Ba<sub>0.4</sub>Sr<sub>0.4</sub>Ca<sub>0.2</sub>TiO<sub>3</sub> specimens with different amounts of ZrO<sub>2</sub>. All Ba<sub>0.4</sub>Sr<sub>0.4</sub>Ca<sub>0.2</sub>TiO<sub>3</sub> specimens exhibited a dense grain structure, and the grain size decreased with the increasing amount of ZrO<sub>2</sub> because some Zr ions are deposited at grain boundaries and inhibit grain growth. The average grain size in the specimen doped with 3 wt.% ZrO<sub>2</sub> was about 6.8 μm (Lee, *et. al.*, 2003).

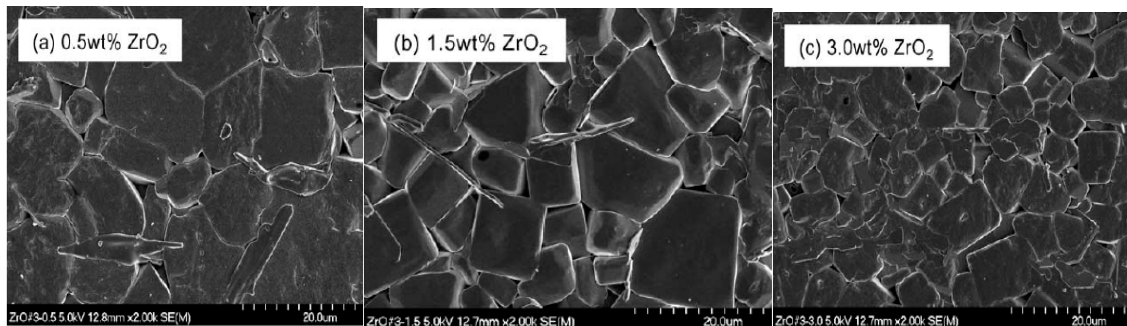


Figure 2.10: Surface microstructures of Ba<sub>0.4</sub>Sr<sub>0.4</sub>Ca<sub>0.2</sub>TiO<sub>3</sub> specimens with various ZrO<sub>2</sub> contents (Lee, *et. al.*, 2003).

Figure 2.11 shows the relative dielectric constant and dielectric loss of  $\text{Ba}_{0.45}\text{Sr}_{0.4}\text{Ca}_{0.15}\text{TiO}_3$  specimen as a function of  $\text{ZrO}_2$  content and temperature at 1 kHz. Increasing the amount of  $\text{ZrO}_2$  resulted in decreasing relative dielectric constant values. This condition happens due to the effect of the decreasing of grain size and substantial replacement of  $\text{Ti}^{4+}$  ion by the  $\text{Zr}^{4+}$  ion in perovskite structure.

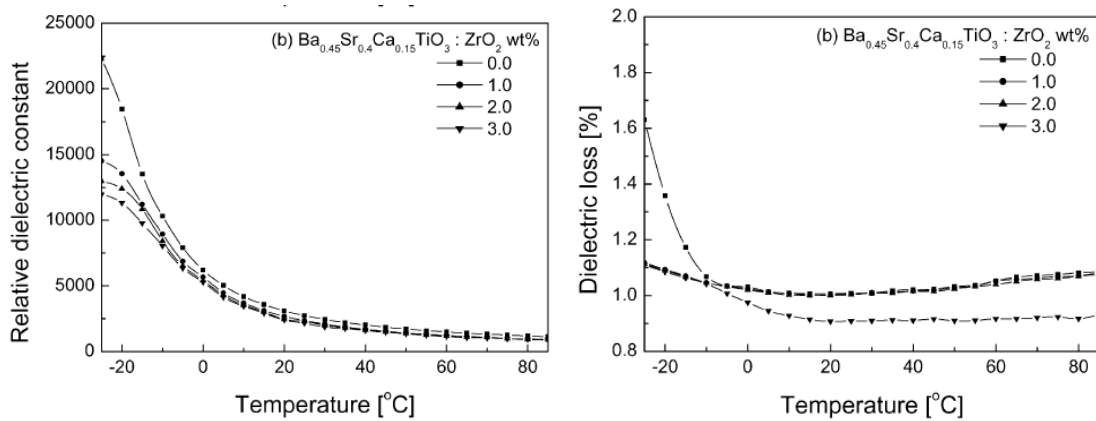


Figure 2.11: Relative dielectric constant and dielectric loss at 1 kHz as a function of temperature for  $\text{Ba}_{0.45}\text{Sr}_{0.4}\text{Ca}_{0.15}\text{TiO}_3$  specimen with various  $\text{ZrO}_2$  contents (Lee, *et. al.*, 2003).

According to Kim, *et. al.*, (2007),  $\text{Si}^{4+}$  doped  $\text{CaCu}_3\text{Ti}_4\text{O}_{12}$  will promotes abnormal grain growth in the ceramic microstructure. The microstructure of  $\text{CaCu}_3\text{Ti}_4\text{O}_{12}$  ceramics changes drastically with only a slight variation in the sintering temperature due to the abnormal grain growth behavior as cited by Adams, *et. al.*, (2002). The change of microstructure significantly alters the dielectric properties.

Abnormal grain growth must be controlled in order to obtain a large and reproducible dielectric constant. Yoon, *et. al.*, (2003) reported that the presence of intergranular liquid for enhanced mass transfer is one important parameter that should be

controlled in abnormal grain growth. With the addition of 2 wt.%  $\text{SiO}_2$ , the abnormal grain growth starting temperature decreased from 1100 to 1060 °C and the temperature for obtaining a uniform and coarse microstructure decreased from 1140 to 1100 °C.

The lowering of the abnormal grain growth temperature by  $\text{SiO}_2$  addition was attributed to the formation of a  $\text{CuO-SiO}_2$ -rich intergranular phase at lower temperature. The apparent dielectric permittivity of coarse  $\text{SiO}_2$ -doped  $\text{CaCu}_3\text{Ti}_4\text{O}_{12}$  ceramics was 10 times higher than that of fine  $\text{SiO}_2$ -doped  $\text{CaCu}_3\text{Ti}_4\text{O}_{12}$  ceramics at the frequency of  $10^3$  to  $10^5$  Hz as shown in Figure 2.12. The doping of  $\text{SiO}_2$  to  $\text{CaCu}_3\text{Ti}_4\text{O}_{12}$  ceramics provides an efficient route of improving the dielectric properties via grain coarsening.

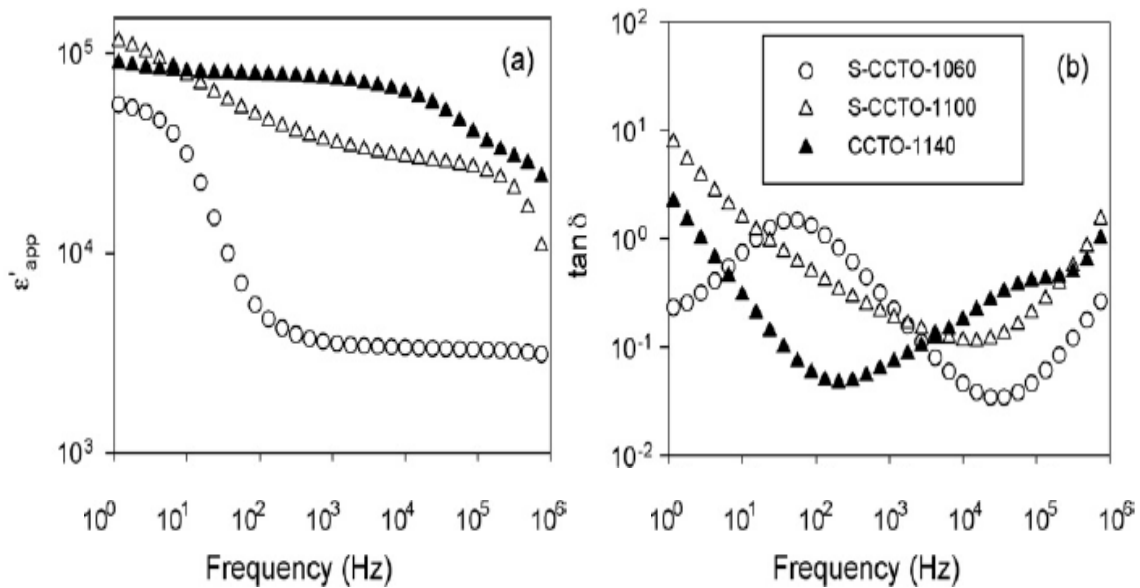


Figure 2.12: (a) Apparent relative permittivity ( $\epsilon'_{app}$ ) (b) loss tangent ( $\tan \delta$ ) of pure and 2 wt.%  $\text{SiO}_2$  doped- $\text{CaCu}_3\text{Ti}_4\text{O}_{12}$  specimens: S-CCTO-1100 (2 wt.%  $\text{SiO}_2$  doped, sintered at 1100 °C for 12 hours); S-CCTO-1060 (2 wt.%  $\text{SiO}_2$  doped, sintered at 1060 °C for 12 hours); CCTO-1140 (pure, sintered at 1140 °C for 12 hours) (Yoon, *et. al.*, 2003)

#### 2.5.4.2 Acceptor Dopants

Ion which known as acceptor dopants is an ion that has a lower charge than the ion they replaced. Most of the time these will be B site ions (substituting for Ti) and the solubility is usually limited to a few tenths of a percent. Acceptor dopants such as  $\text{Mn}^{2+,3+}$ ,  $\text{Co}^{2+,3+}$ ,  $\text{Fe}^{2+,3+}$ ,  $\text{Ni}^{2+}$  and  $\text{Zn}^{2+}$  induce vacancies in the oxygen sublattice in order to balance charge. These oxygen vacancies promote the potential for electrolytic migration of oxygen ions when a strong direct current (dc) bias voltage is applied. In most oxides, the oxygen ions are usually less mobile than cations, thus a dopant favoring an increase in the oxygen vacancy may promote densification.

Kobayashi *et. al.* (2003) cited that 2 % substitution of  $\text{Mn}^{3+}$  for  $\text{Cu}^{2+}$  in  $\text{CaCu}_3\text{Ti}_4\text{O}_{12}$  dramatically quenches the huge  $\epsilon$  of  $10^4$  down to 100 over the measured temperature range from 4.2 to 300 K. This study also determines value of  $\epsilon$  for  $\text{CaCu}_3\text{Ti}_4\text{O}_{12}$  at frequency 1 MHz at 300 K is  $\sim 10000$ . The result as shown in Figure 2.13 emphasize that only 2 %  $\text{Mn}^{3+}$  substitution dramatically suppresses  $\epsilon$  over the measured temperature range from 4.2 to 300 K.

The present of impurity in usual substitution induces a tiny change in  $\epsilon$  due to dipole moment responds to an external field. Kobayashi *et. al.* (2003) suggested that reason of results in Figure 2.13 is the dipole moments interact to respond in a collective way, and that a small amount of impurity suppresses the collective motion. Such a collective motion usually causes a ferroelectric transition, but in the present material the robust cubic structure suppresses the ferroelectric transition, holding the degeneracy of the ferroelectric domain.